Visible-light absorption and large band-gap bowing of GaN_{1−x}Sb_{x} from first principles

R. Michael Sheetz, Ernst Richter, Antonis N. Andriotis, Sergey Lisenkov, Chandrashekhar Pendyala, Mahendra K. Sunkara, and Madhu Menon

Phys. Rev. B **84**, 075304 — Published 1 August 2011

DOI: 10.1103/PhysRevB.84.075304

Visible light absorption and large band gap bowing in dilute alloys of gallium nitride with antimony

R. Michael Sheetz*

Center for Computational Sciences,

University of Kentucky, Lexington, KY 40506-0045

Ernst Richter†

Daimler AG GR/PSS, Wilhelm-Runge-Str. 11, 89081 Ulm, Germany

Antonis N. Andriotis‡

Institute of Electronic Structure and Laser, FORTH,

P.O. Box 1527, 71110 Heraklio, Crete, Greece

Sergey Lisenkov§

Department of Physics, University of South Florida Tampa, FL 33620-5700

Chandrashekhar Pendyala and Mahendra K. Sunkara¶

Conn Center for Renewable Energy Research and Chemical Engineering Department,

University of Louisville, Louisville, KY 40292

Madhu Menon**

Department of Physics and Astronomy,

University of Kentucky, Lexington, KY 40506-0055

Center for Computational Sciences,

University of Kentucky, Lexington, KY 40506-0045

Abstract

Applicability of the $Ga(Sb_x)N_{1-x}$ alloys for practical realization of photoelectrochemical water splitting is investigated using first-principles density functional theory incorporating the LDA/GGA+U formalism. Our calculations reveal that a relatively small concentration of Sb impurities is sufficient to achieve a significant narrowing of the band gap, enabling absorption of visible light. Theoretical results predict that $Ga(Sb_x)N_{1-x}$ alloys with 2 eV band gap straddles the potential window at moderate to low pH values thus indicating that dilute $Ga(Sb_x)N_{1-x}$ alloys as potential candidates for splitting water under visible light irradiation.

PACS numbers: 71.20.-b,73.20.Hb,75.30.Et,75.30.Hx

*Electronic address: rmshee0@email.uky.edu

†Electronic address: ernst.richter@daimler.com

‡Electronic address: andriot@iesl.forth.gr

§Electronic address: slisenk@cas.usf.edu

¶Electronic address: mahendra@louisville.edu

**Electronic address: madhu.menon@uky.edu

Ternary semiconductors are potential candidates for opto-electronic and photoelectrochemical (direct solar water splitting) applications owing to their tunable composition dependent properties. Solar water splitting requires the material to have a band gap between 1.7 eV and 2.2 eV and the band edges to straddle H_2/O_2 redox potentials. Gallium Nitride (GaN), a wide, direct band gap semiconductor, has been shown to be stable under visible photolysis and has the right band edge energetics[1]. Tandem cells based on III-V materials have been shown to have very high efficiency for spontaneous photoelectrochemical (PEC) water splitting ($\approx 12\%$)[2], but their applicability as single gap cells for direct photoelectrochemical water splitting has been limited by the unfavorable band energetics[3]. The successful development of photocatalysts, which work under visible light irradiation to efficiently utilize solar energy, has remained elusive.

Recently, a solid solution between GaN and ZnO, $(Ga_{1-x}Zn_x)(N_{1-x}O_x)$ with $0.05 < x < 0.22$, has been shown to be a promising candidate for overall water splitting[4]. This solid solution is found to be stable during the overall water splitting reaction in contrast to the conventional non-oxide photocatalysts, such as CdS. More importantly, this alloy system is found to be more favorable than the superlattice system in terms of light absorption in the longer-wavelength regions. Band gap reduction in this non-isovalent system has been calculated theoretically[5] but the best achieved band gap reduction for these alloys experimentally is 2.6 eV[6] which makes the material an inefficient solar light absorber. Further studies have suggested that increasing the Zn content in this alloy can improve the photocatalytic activity of this solid solution[7, 8]. Band gap reduction of almost 1 eV has also been achieved in $ZnO_{1-x}Se_x$ alloys[9] with Se substitutional composition x <0.12, although the stability of this alloy has not been investigated in detail. Similar to ZnO, there is a significant interest in developing alloys based on GaN for obtaining the suitable material for solar water splitting due to stability and band edge energetics considerations.

Currently, $In_xGa_{1-x}N$ is the most widely studied material system where about 30% In incorporation is required to get to the required band gap. Reports indicate that such excess In contents leads to phase segregation. By contrast very little attention has been focused on dilute nitride antimonides, such as GaN_xSb_{1-x} in the mid band gap composition. The experimental results reported for the latter are very few[9, 10]. GaN is a wide band gap material with a fundamental band gap of ≈ 3.4 eV[11]. Although this gap corresponds to wavelengths below the visible, substitutional doping with Sb is expected to bring this down

to the required value. Reports have shown that dilute ternary alloys for the GaN_xSb_{1-x} system for even a very small x value shows band gap bowing that has been extended to negative band gaps for composition in excess of about 8% N[12]. Following the same trend it is reasonable to expect that a similar concentration of Sb incorporation into GaN may be sufficient to get to the desired composition range.

In this work, using first principles calculations, we provide evidence for an anomalous decrease in the electronic band gap in GaN with the substitutional doping by Sb. In particular, we show that band gap reduction for enabling absorption in the visible can be achieved even at Sb concentration as low as $x = 0.05$. The system becomes a semi-metal at Sb concentration $x > 0.06$.

First principles density functional theory (DFT) based on the local density approximation (LDA) and generalized gradient approximation (GGA) are performed with Cambridge Serial Total Energy Package (CASTEP)[13] as implemented in the Materials Studio software package (Accelrys Software Inc.). The ultra-soft pseudopotential[14] is employed for electron-ion interaction. Even though LDA/GGA formalism suffers from the well known "gap problem", incorporation of the Hubbard parameter, U, in the formalism (LDA/GGA+U method) helps alleviate this problem [15, 16]. The U parameter is an on-site Coulomb repulsion parameter that incorporates part of the electron correlation absent in LDA/GGA. The U values thus obtained are: $U_{s,N}$=19.25 eV and $U_{s,Sb}$=0.40 eV. All other U values such as $U_{d,Ga}$, $U_{p,Ga}$, $U_{s,Ga}$, $U_{p,N}$ and $U_{p,Sb}$ are set to zero. These values of U reproduce the experimental band gaps of bulk GaN (3.43 eV[17]) and GaSb (0.73 eV[18]). We use this GGA+U method to calculate the band structure, density of states (DOS), and optical properties. All self-consistent calculations were carried out using a convergence criterion of 10^{-6} eV. The geometric structures in all cases were optimized using GGA and the Perdew-Burke-Ernzerhof (PBE) correlation functional prior to performing the GGA+U calculations. Spin-polarized GGA+U calculations were carried out using an energy cutoff of 600 eV. The optical spectra are obtained by calculating the imaginary part of the complex dielectric function from the matrix elements of the position operator between occupied and unoccupied states within the spin-polarized GGA + U method as implemented in CASTEP. The allowed transitions are determined by the nonzero matrix elements of the position operator. For optical properties it is essential to use sufficient number of $k-$ points in the calculations of matrix elements. We use a $5\times5\times5$ $k-$point grid. It is also important to have sufficient number of conduction

bands for accuracy. We have employed 100 empty bands in our calculations. Convergence criteria has been verified by testing the changes in optical properties with respect to the number of $k-$points and conduction bands.

We consider bulk GaN in the wurtzite structure simulated by a relatively large 72 atom supercell with periodic boundary conditions. $Ga(Sb_x)N_{1-x}$ structures are obtained by substituting up to 3 N atoms with Sb. In each case considered both the cell volume as well as the individual atomic positions have been fully optimized without any symmetry constraints. We also considered bulk GaSb zinc-blende structure in the form of a 48 atom supercell and studied the effects of N substitution to obtain $Ga(N_x)Sb_{1-x}$ structures. In Fig. 1 we show the optimized supercells of GaN with 2 substitutional Sb (left) and GaSb with 2 substitutional N (right).

In order to check the thermal stability of the $Ga(Sb_x)N_{1-x}$ structures, we performed *ab initio* molecular dynamics (MD) simulations on the Born-Oppenheimer potential surface using the Plane-Wave Self-Consistent Field (PWSCF) code of the QUANTUM-ESPRESSO package[19]. The interatomic forces have been calculated using the Hellmann-Feynman theorem on the self-consistent electronic ground state at each time step, described by the DFT electronic structure, solving the equations of motion with an integration time step of 1 femto second (fs). The simulation time of each trajectory is more than 2 pico seconds and it is enough to explore the structural changes. Taking into account the fact that these types of alloys are usually synthesized at temperatures near 500 C, we performed constant temperature MD simulations using the Berendsen thermostat[20] to control the temperature of the $Ga(Sb_x)N_{1-x}$ structures at 800 K starting from the corresponding structures optimized using CASTEP. No dissociation of the structures were found indicating that the proposed alloys are thermally stable.

We next perform electronic structure analysis of optimized $Ga(Sb_x)N_{1-x}$ and $Ga(N_x)Sb_{1-x}$ structures. For the $Ga(Sb_x)N_{1-x}$ structures there is a monotonic increase in the lattice parameters with an increase in x on relaxation. Similarly, for the $Ga(N_x)Sb_{1-x}$ structures there is a monotonic decrease in the lattice parameters with an increase in x on relaxation. The structural optimizations result in considerable local distortions in $Ga(Sb_x)N_{1-x}$ and $Ga(N_x)Sb_{1-x}$ cases due to the size and electronegativity mismatch between N and Sb. Rapid decrease in the band gap is seen with an increase in the dopant concentration for the $Ga(Sb_x)N_{1-x}$ system. Fig. 2 shows the electronic band gap as a function of the fraction, x,

for $Ga(Sb_x)N_{1-x}$ and $Ga(N_x)Sb_{1-x}$ alloys. In all $Ga(Sb_x)N_{1-x}$ cases considered, the gaps are direct. The figure also lists the experimental band gaps of $Ga(N_x)Sb_{1-x}$ for $x = 0.015$[10, 21] and $x = 0.017$[22] for comparison. In the case of the $Ga(Sb_x)N_{1-x}$ alloy the rapid closing of the gap for $x > 0.06$ is worth noting. The band gap value of 2 eV found for $0.05 < x < 0.06$ is ideal for PEC water splitting.

The large band gap reduction appears to be an important feature of the HMAs[23]. The most widely studied HMAs comprise III-V host with isovalent N and As substituting group V anions. A number of models have been proposed to explain the band gap reduction in these materials. The most successful model to explain this phenomena has been the so called band anticrossing (BAC) model. The BAC model takes into account an anticrossing interaction between localized states of the substitutional isovalent anion atoms and the extended states of the host III-V semiconductor matrix. Depending on whether the impurity level is coupled to the host conduction band or to the host valence band, the BAC model will be referred to as conduction-BAC (CBAC) and valence-BAC (VBAC) model, respectively. In particular, the VBAC model has been used to explain band gap reduction in a number of HMAs[24].

The defect states of large-sized impurities with first ionization energies less than that of the host anion often lie near the valence-band edge of the host semiconductor. Antimony is among the largest of the group V elements and its energy levels are near and below the VBM of GaN. The anticrossing interaction results in band splitting and the restructuring of the VBM which is shifted upward leading to a reduction in the energy gap. Increasing Sb concentration pushes the VBM up at a rapid rate while the conduction bands move down at a slower rate. In Fig. 3 we show the electronic band structure and projected density of states (PDOS) for the geometry shown in Fig. 1, left for $0.05 < x < 0.06$. The valence band splitting is evident in the figure. Also, as seen in the PDOS, the valence bands responsible for the narrowing of the gap derive their contribution from the p states of Sb and the extended s and p states of the host.

The band gap of 2 eV obtained for $0.05 < x < 0.06$ in Fig. 3 opens up the exciting possibility of visible absorption for the $Ga(Sb_x)N_{1-x}$ alloys. The allowed optical transitions across the band gap predicted by the calculation of optical properties for the Sb concentration, $0.05 < x < 0.06$, are indicated by the arrows in Fig. 3. For the [0,1,0] orientation of the incident light there appears to be two absorption frequencies in the visible with one of them connecting the conduction band minimum and the valence band maximum at the zone

center. Allowed absorptions in the visible are also obtained for other incident directions.

The applicability of the $Ga(Sb_x)N_{1-x}$ alloys for practical realization of direct PEC water splitting is illustrated in the band offset diagram in Fig. 4. The band edges of GaN, GaSb and InN are indicated[25] along with the trends in band edge variations of the corresponding alloys. The energy scales on the Y-axis are plotted with respect to S.H.E (standard hydrogen electrode) and vacuum scale. The conversion used for the scales is given by the relation E (SHE) + E (vac) = - 4.44[26]. The H_2/O_2 redox potentials are indicated for pH 4 as a reference.

InN has almost linear variation in band gap with composition and the solid lines indicate the same. It can be observed that $In_x(Ga_{1-x})N$ alloys with 2.7 eV band gap have the conduction band edge positive of the H_2 potential. Hence, the 2 eV band gap alloy in the mid composition range will not straddle the H_2/O_2 potential window making direct unassisted water splitting impossible. Alloying fraction on the X-axis is plotted only in the dilute nitrogen ($\leq 10\%$) and dilute antimony ($\leq 10\%$) regions. The trend for $Ga(Sb_x)N_{1-x}$ in the dilute nitrogen region (indicated by the dash-dot line) is plotted incorporating the reported band gap bowing in dilute nitride $Ga(Sb_x)N_{1-x}$ alloys. The vertical lines in the dilute antimony region indicate the band gaps of different alloy compositions calculated in this work. Majority of the shift in band edge positions is due to antimony incorporation hence, the valence band edge moves up considerably for each of the three calculated alloy compositions $x = \frac{1}{36}, \frac{2}{36}$ and $\frac{3}{36}$, while the the conduction band edges are moved down by smaller amounts. The dashed line indicates the calculated trend of band edge variation. From the band edge positions, it is clear that $Ga(Sb_x)N_{1-x}$ alloy with $x = 0.056$ ($\approx$2 eV band gap) straddles the potential window. Estimates show that the material straddles the potential window at moderate (8) to low (1) pH values.

GaN is also known to have high corrosion stability. The relatively small addition (2.8%) of antimony is not expected to create a significant change in the corrosion resistance of the material. Our initial simulation results show that dilute antimonide $Ga(Sb_x)N_{1-x}$ alloys are promising materials for PEC water splitting applications. Further investigation by way of rigorous simulations supported by experimental data is needed to explore and understand this material system. $Ga(Sb_x)N_{1-x}$ system could also be an alternative to the $(ZnO)_{1-x}(GaN)_x$ solution that has shown some promise for overall water splitting since the latter could suffer from charge imbalance resulting from non isovalent substitutions of Ga

with Zn and N with O. In particular, if the N atom is in a position far away from the Ga atom in ZnO matrix, local defect centers would be created resulting in charge recombination centers which could adversely affect the efficiency of PEC water splitting[5].

The present work is supported through grants by DOE (DE-FG02-00ER45817 and DE-FG02-07ER46375).

---

[1] A. Beach, R. T. Collins, and J. A. Turner, J. Electrochem. Soc. **150**, A899 (2003).

[2] O. Khaselev and J. A. Turner, Science **280**, 425 (1998).

[3] T. G. Deutsch, C. A. Koval, and J. A. Turner, J. Phys. Chem. **110**, 25297 (2006).

[4] D. Lu, T. Takata, N. Saito, Y. Inoue, and K. Domen, Nature **440**, 295 (2006).

[5] M. N. Huda, Y. Yan, S. H. Wei, and M. M. Al-Jassim, Phy. Rev. B **78**, 195204 (2008).

[6] K. Maeda, K. Teramura, T. Takata, M. Hara, N. Saito, K. Toda, Y. Inoue, H. Kobayashi, and K. Domen, J. Phys. Chem. B **109**, 20504 (2005).

[7] H. Chen, L. Wang, J. Bai, J. C. Hanson, J. B. Warren, J. T. Muckerman, E. Fujita, and J. A. Rodriguez, J. Phys. Chem. C. **114**, 1809 (2010).

[8] L. L. Jensen, J. T. Muckerman, and M. D. Newton, J. Phys. Chem. C. **112**, 3439 (2008).

[9] K. Nunna, S. Iyer, L. Wu, J. Li, S. Bharatan, X. Wei, R. T. Senger, and K. K. Bajaj, J. Appl. Phys **102**, 053106 (2007).

[10] T. D. Veal, L. F. J. Piper, S. Jollands, B. R. Bennett, P. H. Jefferson, P. A. Thomas, C. F. McConville, B. N. Murdin, L. Buckle, G. W. Smith, et al., Appl. Phys. Lett. **87**, 132101 (2005).

[11] B. Monemar, Phys. Rev. B **10**, 676 (1974).

[12] A. Belabbes, M. Ferhat, and A. Zaoui, Appl. Phys. Lett. **88**, 152109 (2006).

[13] M. D. Segall, P. J. D. Lindan, M. J. Probert, C. J. Pickard, P. J. Hasnip, S. J. Clark, and M. C. Payne, J. Phys. Cond. Matter. **14**, 2717 (2002).

[14] D. Vanderbilt, Phys. Rev. B. **41**, 7892 (1990).

[15] A. Walsh, J. L. F. DaSilva, and S.-H. Wei, Phys. Rev. Lett. **100**, 256401 (2008).

[16] N. N. Lathiotakis, A. N. Andriotis, and M. Menon, Phy. Rev. B **78**, 193311 (2008).

[17] I. Vurgaftman and J. R. Meyer, J. Appl. Phys. **94**, 3675 (2003).

[18] A. Chandola, R. Pino, and P. S. Dutta, Semicond. Sci. Technol. **20**, 886 (2005).

[19] S. Baroni, A. D. Corso, P. G. S. de Gironcoli, C. Cavazzoni, G. Ballabio, S. Scandolo, G. Chiarotti, P. Focher, K. L. A. Pasquarello, A. Trave, et al., QUANTUM-ESPRESSO package (http://www.quantum-espresso.org/) (2005).

[20] H. J. C. Berendsen, J. P. M. Postma, W. F. van Gunsteren, A. DiNola, and J. R. Haak, J. Chem. Phys. **81**, 3684 (1984).

[21] L. Buckle, B. R. Bennett, S. Jollands, T. D. Veal, N. R. Wilson, B. N. Murdin, C. F. McConville, and T. Ashley, Journal of Crystal Growth **278**, 188 (2005).

[22] A. Mondal, T. D. Das, N. Halder, S. Dhar, and J. Kumar, Journal of Crystal Growth **297**, 4 (2006).

[23] J. Wu, W. Shan, and W. Walukiewicz, Semicond. Sci. Technol. **17**, 860 (2002).

[24] W. Shan, W. Walukiewicz, K. M. Yu, J. Wu, J. W. I. Ager, E. E. Haller, H. P. Xin, and C. W. Tu, Appl. Phys. Lett. **76**, 3251 (2000).

[25] C. G. V. de Walle and J. Neugebauer, Nature **423**, 626 (2003).

[26] A. J. Bard, R. Memming, and B. Miller, Pure and Appl. Chem. **58**, 955 (1986).

Figures

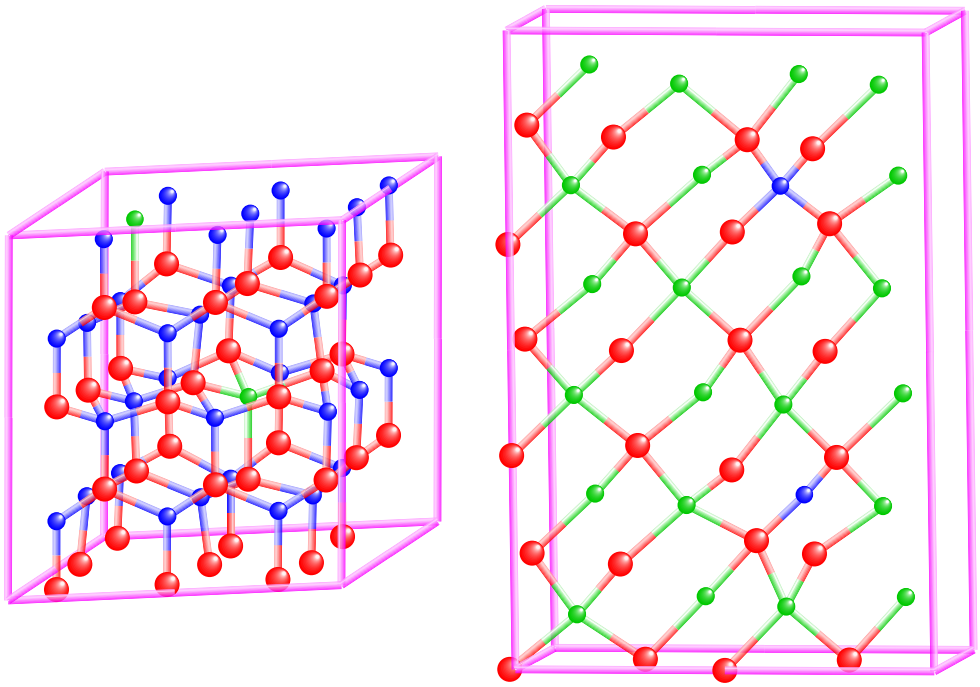

FIG. 1: The optimized supercells of GaN with 2 substitutional Sb (left) and GaSb with 2 substitutional N (right).

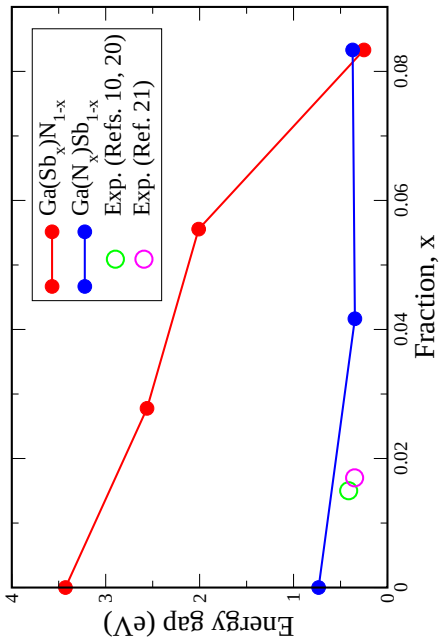

FIG. 2: The calculated band gaps for $Ga(Sb_x)N_{1-x}$ and $Ga(N_x)Sb_{1-x}$ alloys as a function of concentration x. For comparison we have also included the experimental band gaps of $Ga(N_x)Sb_{1-x}$ for $x = 0.015$[10, 21] and $x = 0.017$[22].

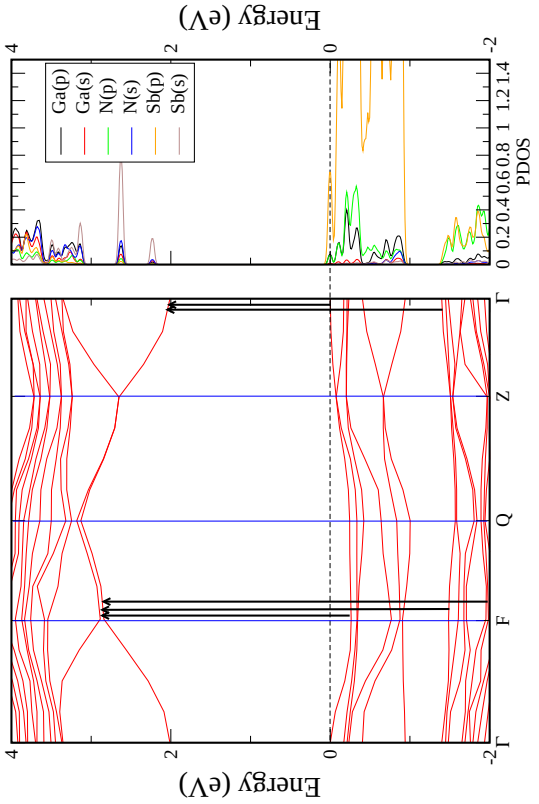

FIG. 3: Calculated band structure, PDOS and allowed optical transitions for the $Ga(Sb_x)N_{1-x}$ alloy shown in Fig. 1, left.

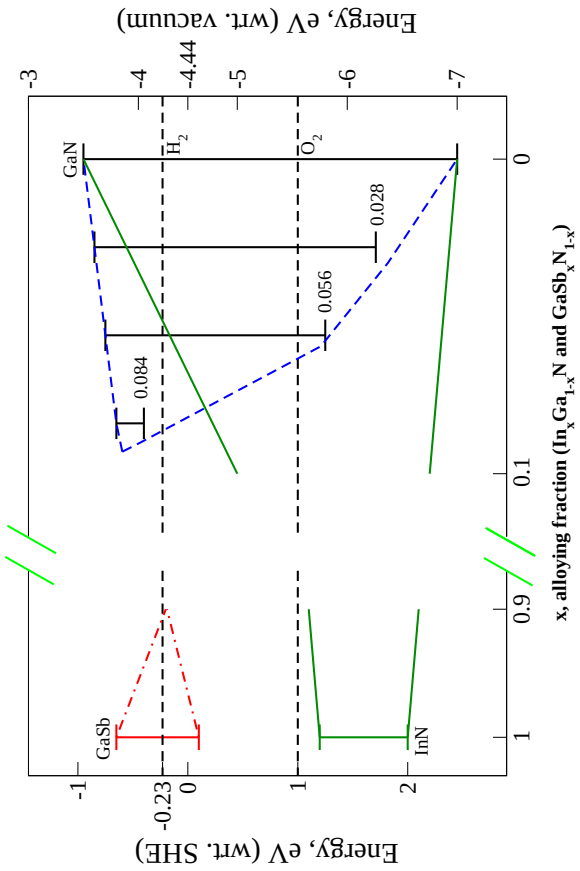

FIG. 4: A qualitative comparison of the band edges of $In_x(Ga_{1-x})N$ and $Ga(Sb_x)N_{1-x}$ alloys is presented. The almost linear band edge variation in $In_x(Ga_{1-x})N$ alloys is indicated by the solid green line. The projected band edge variation of $Ga(Sb_x)N_{1-x}$ is plotted using the reported band gap values for dilute nitrogen alloys, indicated by the dash-dot line. The band edge and band gap positions calculated in this work are indicated by the vertical lines and the variation is plotted as indicated by the dashed lines emerging from GaN band edges. It is evident that $Ga(Sb_x)N_{1-x}$ alloy with 2 eV band gap straddles the H_2/O_2 redox potential window and that very low Sb incorporation is sufficient to reduce the band gap of $Ga(Sb_x)N_{1-x}$ alloys from UV to the visible region.